Hindawi
International Transactions on Electrical Energy Systems
Volume 2024, Article ID 3559456, 18 pages
https://doi.org/10.1155/2024/3559456

Research Article

A Grey-Box Model of a DC/DC Boost Converter for PV Energy Systems

Kerim Karabacak

Kutahya Dumlupinar University, Kutahya Technical Sciences Vocational School, Department of Electronics and Automation, Kutahya, Türkiye

Correspondence should be addressed to Kerim Karabacak; kerim.karabacak@dpu.edu.tr

Received 28 September 2023; Revised 15 January 2024; Accepted 14 March 2024; Published 20 March 2024

Academic Editor: Mahdiyeh Eslami

This paper presents a grey-box model of a DC/DC boost converter for PV energy systems. The proposed model contains a white-box model part and a black-box model part together to prepare a better model for the PV boost converter. The white-box model part is used for knowledge of the circuit by mathematical equations since the black-box model part is used for unknown parameters such as temperature and electromagnetic interference. The black-box part of the proposed model is created by a nonlinear system identification of a real boost converter circuit with an artificial neural network. The precision of the mathematical model and the advantages of the fast prediction ability of the artificial neural network were used together. The proposed grey-box model is compared with the existing state-space and black-box models and experimental results. The results of the study showed that the average correlation between the proposed grey-box model output and the experimental results is 97.52%. Therefore, the proposed model can be used for analyzing DC/DC boost converter output characteristics before field applications.

1. Introduction

1.1. Background. Photovoltaic (PV) energy systems are taking an important role in energy production systems due to their clean energy production process. However, improving PV energy system efficiency is a big issue. For this reason, there are many studies about improving PV cell technology. However, another way to increase PV system efficiency is by improving the efficiency of the power electronics circuits used in PV energy systems. Since DC/DC boost converters are one of the most commonly used power electronic circuits in PV energy systems, efficiency improvements of DC/DC boost converters directly affect the efficiency of PV energy systems. To increase the efficiency of DC/DC converters used in PV energy systems, the working principle and the behavior of the circuit should be well known. So accurate modeling of DC/DC boost converters for PV energy systems is a good way to understand circuit behavior before field applications.

Commonly, DC/DC converters are modeled with deterministic models such as mathematical equations. However, mathematical equations are not adequate to express the transient output voltage changes of the circuit. So to understand the input-output relation of the circuit better, black-box models are used in various types of DC/DC converters. Black-box models are used to obtain parameters that cannot be expressed mathematically by identification. However, in some situations, black-box models can have uncertain output behavior when input-output data are poor. So when some mathematical equations of the system are known, using a grey-box model is a better way to model a dynamic system instead of using a black-box model. A grey-box model is described as a combination of a white-box model part and a black-box model part. The white-box model part is based on mathematical equations since the black-box model part is created by nonlinear identification of the uncertain system parameters by using an input-output dataset.

1.2. Literature Review. In the literature, there are various studies about the grey-box modeling of energy systems.

Zhao et al. [1] used the grey-box method for online monitoring of DC-link capacitors. The authors stated that the damping factor α (related to capacitance) of the large-signal transient trajectories of converters is a new health indicator for capacitors. Based on this, the model realizes the condition monitoring of DC-link capacitors with minimum dependency on the detailed topology and control information. According to experimental results, the estimation errors of the damping factor and DC-link capacitance were found to be less than 1%.

Ungerland et al. [2] introduced a grey-box technique for consolidating active distribution networks that incorporate grid-forming converters. Their method relies on voltage sensitivities to depict the grid's resilience at the connection point of the grid-forming converter. The resulting aggregated model effectively replicates the intricate dynamic characteristics of the original network. Consequently, their grey-box method offers a substitute equivalent model capable of replacing detailed distribution network models.

Roosta et al. [3] put forward an adaptive neuro linear quadratic regulator (ANLQR) controller designed specifically for buck converters functioning in environments with disruptive disturbances. Their investigation centers on the integration of a neural network to refine and adjust the gain of the linear quadratic regulator (LQR) approach by using an adaptive mechanism. This approach operates under the premise that the system can be treated as a grey-box process, obviating the requirement for an exact mathematical model, which can lead to reduced computational demands, swifter system response, and simpler implementation.

Rosati et al. [4] conducted a study exploring system identification (SI) and data-driven modeling methods as substitutes for deriving models from fundamental principles in the context of modeling a vented oscillating water column wave energy converter. Their findings suggest that SI models offer a degree of adaptability, as they can either rely solely on data (referred to as black-box models) or integrate some level of physics-based insights (referred to as grey-box models). Their research demonstrates that when the converter system is regarded as a grey-box model, metaheuristic algorithms can be effectively employed for targeted design within this framework.

Wang et al. [5] highlighted that viewing a converter system as a grey-box model allows for the implementation of metaheuristic algorithms for targeted design within this framework. Consequently, they introduced a genetic algorithm (GA) applied to the parametric design of the dual active bridge (DAB) converter. Their approach included an explicit fitness criterion aimed at identifying and mitigating the high-frequency oscillation (HFO) issue. Through comparative experiments, they demonstrated the efficacy of their method, achieving a 4% enhancement in efficiency with a power delivery of 200 W, particularly through the tuning of the splitting inductance.

Liu et al. [6] introduced two Bayesian methodologies: semiconjugate linear regression and noisy input Gaussian process regression. These techniques serve for both parametric and nonparametric modeling in the context of grey-box and black-box modeling. Their findings illustrate that the proposed approaches for system identification of ships and wave energy converters (WECs) exhibit strong generalization capabilities and robustness.

Zong et al. [7] introduced a comprehensive grey-box aggregation model for wind farms along with a parameter identification technique that does not necessitate detailed knowledge of the wind farm internals. They developed a simplified grey-box aggregation model for low-medium and high-frequency ranges and applied a vector fitting-based method to identify its parameters. The resulting aggregation model closely matched the broad frequency characteristics (ranging from 1 to 2500 Hz) of the detailed wind farm, making it suitable for wideband oscillation analysis.

In reference [8], the authors introduced a method for analyzing small-signal stability in grid-tied converter systems, considering both the "white-box" and "black/grey-box" scenarios, accounting for frequency couplings across various operating conditions. Consequently, they identified stable operating regions under different grid impedances, offering valuable insights into ensuring the stability of grid-tied converters.

Hafiz et al. [9] introduced a straightforward approach to grey-box identification for modeling a real DC-DC buck converter operating in continuous conduction mode. Their method, rooted in the concept of term clusters, offers a simplified means to determine the static response of potential models. Essentially, their approach transforms the grey-box identification challenge into a multiobjective framework, aiming to balance the bias-variance trade-off in model construction while incorporating prior knowledge into the structure selection process. Through their investigation focusing on a practical buck converter scenario, they showcased the feasibility of identifying concise models capable of capturing both dynamic and static behaviors across a broad input range.

Hu et al. [10] developed a small-signal model for a variable-speed multigenerator (VSMG), which is comparable to an adapted third-order synchronous generator (SG). The authors used a grey-box system specification in which equivalent electrical parameters were estimated alternately and iteratively to model the synchronous generator (SG). The accuracy of the equivalent SG model in the time domain is confirmed by simulation results.

In reference [11], the authors introduced a dynamic model for active distribution networks that aggregates various generation technologies, considering their anticipated responses in compliance with the latest European grid code requirements, particularly regarding voltage support services. The primary objective of this model and its identification methodology was to accurately represent the transient behavior of the active distribution system following significant voltage disturbances originating from the transmission side. The model's parameters were determined using an evolutionary particle swarm optimization algorithm, which involved comparing the frequency domain responses of active and reactive power flows at the boundary of the transmission-distribution interface substation

between a detailed distribution network model and the aggregated model.

Amin et al. [12] introduced a grey-box approach designed to estimate the parameters of controllers within a wind energy conversion system (WECS), relying on fundamental assumptions regarding the system's control structure. Their method focused on identifying the portions of the equivalent WECS impedance that significantly influence system stability and subsequently adjusting the impedance to promote stability. Their research findings indicated that this method effectively guarantees system stability by readjusting only the crucial controller parameters.

Lee et al. [13] performed a requirements analysis using a grey-box approach and utilized select products from the design phase derived from this analysis. Subsequently, they developed an automation system that converts these products into a system model by using a model converter for use with the model checker.

Mat Zali et al. [14] outlined the creation of a dynamic equivalent model for an active distributed network (ADN) by utilizing the grey-box methodology. Their model comprises a converter-connected generator and a composite load model running in parallel. Opting for the grey-box approach was motivated by its ability to integrate prior knowledge about the ADN structure into the model, rendering it more physically meaningful and intuitive compared to black-box or white-box models. This approach holds promise for enhancing the model's accuracy.

Milanovic et al. [15] introduced an equivalent model for an active distribution network cell (ADNC) featuring distributed generation, intended for studies on transmission system stability. This ADNC model includes a converter-connected generator and a composite load model operating in parallel. They opted for the grey-box approach to model development because it allows for the incorporation of prior knowledge about the ADNC structure, thereby enhancing the model's physical relevance and intuitiveness compared to black-box or white-box models.

In reference [16], the authors outlined a swift calibration method aimed at determining the parameters of a dynamic battery model tailored for automotive applications. This dynamic model adopts a phenomenological approach based on an equivalent circuit model, with parameters varying as linear spline functions of the state of charge (SoC). The model identification process follows a layered approach: a two-step optimization procedure utilizing a genetic algorithm (GA) is employed to fine-tune the model parameters across an experimental dataset covering the pertinent operating conditions for the batteries. The authors successfully applied this process to both lithium-ion and NiMH chemistries, yielding favorable outcomes.

Arahal et al. [17] developed a thermal storage tank model by employing the simultaneous perturbation stochastic approximation technique to fine-tune the parameters of a serial grey-box model structure. The advantages of this approach are discussed within the context of its intended application, which necessitates a model capable of accurately simulating the storage tank's behavior while imposing minimal computational burden and maintaining low error levels over medium to large timeframes. The model underwent testing against real-world data across various scenarios, evaluating its performance in terms of simulation accuracy for temperature profiles and the amount of usable energy stored in the tank. The results obtained affirm the effectiveness and practicality of the proposed approach.

In reference [18], the authors explored the practical utility of artificial neural networks (ANNs) for constructing measurement-based continuous-time dynamic equivalents for power systems. Their methodology involves utilizing measurements taken at boundary nodes between a subsystem earmarked for detailed modeling (the "retained" portion) and the segment slated for replacement with a simplified ("equivalent") model. Their approach blends conventional physics-based models with signal-based models derived from measurements. To categorize these models, they employ a color-coding scheme, distinguishing between physics-based models (termed clear or white box) on one end, signal-based models (referred to as opaque or black box) on the opposite end, and hybrid (grey box) models in between.

In reference [19], the authors adopted a grey-box methodology employing parameter estimation for NARMAX polynomial models applied to a practical DC-DC buck converter. While the static relationship was theoretically understood, the identification data were limited to a narrow range around an operating point. Despite being derived from dynamic data, their models effectively approximated the nonlinear static function, offering a promising outcome.

Aguirre et al. [20] explored the integration of prior knowledge regarding the system's static nonlinearity into the model, highlighting the trade-off between accurately estimating the model's static nonlinearity and the quality of predictions, especially in applications involving nonlinear systems. They applied these concepts to identify a real DC-DC buck converter operating continuously. By incorporating straightforward prior information that considers the steady-state voltage relation of the converter, they achieved an enhancement in the overall stability of the model. These models, which are valid across a broad operational spectrum, are concise and can be directly estimated using data obtained from the converter.

1.3. Research Gap and Motivation. As mentioned above, there are some studies about grey-box modeling used in various energy systems. However, there are few studies about the grey-box modeling of DC/DC converter circuits. These few studies are mostly about buck converters. On the other hand, for renewable energy systems, especially PV energy systems, boost converter circuits are one of the most preferred power electronic circuits. In PV energy systems, DC/DC boost converter circuits are used to adjust the preinverter voltage. Also, they are used as voltage stabilizers when DC loads are directly connected to PV panels. Another usage of DC/DC boost converters is maximum power point tracking (MPPT) applications for charging batteries. Therefore, the voltage input-output behavior of DC/DC

boost converters should be well-known before field applications. The subject of developing innovative models for boost converter circuits, which is so important to be used in renewable energy systems, has remained missing in the literature. Detailed, effortless, and realistic modeling of DC/DC boost converters is revealed as a research gap in the literature. So models used for simulations of DC/DC boost converters used in renewable energy systems need to be improved.

The different aspect of this study from other studies in the literature is that the boost converter circuit is modeled using the grey-box modeling method. So the proposed model contains both the advantages of deterministic mathematical modeling and system identification. The proposed model consists of a state-space white-box part that comes from physical knowledge of the boost converter and a black-box identification part by artificial neural networks (ANNs) for the addition of system dynamics which is difficult to express mathematically.

In solar energy and wind energy systems, MPPT algorithms adjust the PV output voltage with DC/DC boost converter circuits and ensure that the maximum power that can be drawn from the PV panel is transferred to the load or battery. In order for MPPT algorithms to work without errors, the boost converter simulation model used in the design phase of the algorithm must be realistic. So the main objective of this paper is to make a realistic model for existing boost converter circuits. So this model will be able to be used to simulate boost converter circuits for PV renewable energy systems before field applications. Also, in the future, better MPPT controller designs can be made by using the proposed grey-box model of DC/DC boost converters, since the input-output relationship of the boost converter circuits can be expressed more clearly than existing mathematical models.

This study also aims to prepare a foundation for speeding up the output voltage stabilization process and robust control of PV renewable energy systems. As a result, it is anticipated that a chain reaction will occur in which a better system model will pave the way for more powerful controller designs.

1.4. Challenges. In DC/DC boost converters used in PV renewable energy systems, the main issue to be controlled is the output voltage level. The controller in the PV renewable energy system decides what the converter output voltage should be by observing the input voltage and produces a duty cycle signal appropriate to this value. The existing state-space model of the boost converter is based on mathematical equations. In the existing mathematical model, excessive fluctuations in the output voltage appear that do not exist in reality. The reason for that should be the system dynamics caused by the magnetic field, temperature, and EMI stress do not exist in the existing state-space model. Since the controller in the system is designed according to the existing deterministic model of the boost converter, the controller may produce a control signal different from what it should be at various times. On the other hand, in real applications, it takes longer for the control system to fix the control signal. This drawback is tried to be encountered by black-box modeling in earlier studies in the literature. However, black-box models have an obstacle in that they do not have sufficient results when training data are poor. Therefore, in some cases, it may not be possible for control systems to generate the control signal correctly.

So it is seen that a new modeling technique is required for a better understanding of the input-output behavior and transient response of DC/DC boost converter circuits.

1.5. Contribution. This paper primarily focuses on the following key contributions:

(1) This study compensates for the lack of dynamic parameters in the existing mathematical model.

(2) This research focuses on the transient responses of the DC/DC boost converter circuit models. The transient responses of the white-box, black-box, and grey-box models are compared.

(3) The DC/DC boost converter circuit is modeled as closely as possible in terms of the system input-output relationship by the proposed model.

(4) This paper is a preliminary study on designing control systems to be used to stabilize the output voltage of PV energy systems.

(5) A groundwork has been prepared for the MPPT action to be carried out more efficiently.

(6) A more suitable model than existing models has been created to enable feasibility and efficiency analyses of DC/DC boost converter circuits before field applications.

1.6. Paper Organization. The remainder of this paper is organized as follows. In the Introduction section, the purpose of using DC/DC boost converters in PV energy systems is mentioned. Then, a detailed literature review is given. Then, a literature review about grey-box modeling of PV energy systems and grey-box models used in DC/DC converters is given. Then, the purpose of the study and the difference between the study and other studies in the literature are given. In the Methodology section, the proposed grey-box model is presented. Then, the real PV energy system and the prototype boost converter circuit used for the identification are given. In the Simulation Results section, the simulation output of the proposed grey-box model is investigated. In the Experimental Results section, the experimental results of the study and comparative output results of the proposed model and existing model are given. In the Conclusion section, the benefits of the proposed model are explained and the planned improvements of the proposed system in the future are expressed.

2. Methodology

A grey-box model of a DC/DC converter is created for use in photovoltaic renewable energy systems. The proposed grey-box model includes a white-box model and a black-box

model. The white-box model and the black-box model are designed to work in parallel. The white-box model is created using mathematical equations, while an artificial neural network algorithm is used to describe the system dynamics in the black-box model. In the study, a 10 kW DC/DC boost converter is designed and produced. The boost converter is operated with a duty cycle signal with a period of 10 kHz. The produced boost converter circuit is used to define the black-box model. The produced boost converter circuit is connected to the 10 kW solar panel block on the roof of the Ege University Solar Energy Institute and operated at various photovoltaic panel voltages and duty cycles. By processing the obtained data with artificial neural networks, a black-box model within the proposed grey-box model is created. Afterward, the proposed grey-box model is used in simulation tests. Following simulation studies, the model is tested experimentally. Experimental test results and simulation study results are compared.

2.1. Proposed Grey-Box Model for the DC/DC Boost Converter. The proposed grey-box model for the DC/DC boost converter consists of a white-box part which parallels a black-box part. The white-box part consists of the state-space model equations for the boost converter. This part contains well-known electrical information about the boost converter by mathematical equations. On the other hand, the black-box part contains boost converter system dynamics caused by energy storage elements in the converter circuit (inductor and capacitor). The black-box part of the model is obtained by identification of the boost converter circuit with artificial neural networks. The main objective of adding a black-box part to the model is to quickly predict what value the system's output will reach when it becomes stable. Figure 1 shows the proposed grey-box model.

2.1.1. The White-Box Model. Fundamentally, a DC/DC boost converter converts low input DC voltage to a higher output DC voltage. A single-switch boost converter consists of an inductor connected in series with an insulated gate bipolar transistor (IGBT) or a metal oxide field effect transistor (MOSFET) and parallels to a diode and capacitor connected in series. Figure 2 shows a basic single-switch boost converter circuit. The output voltage changes by the duty cycle of the pulse width modulation (PWM) signal applied to the gate of the IGBT/MOSFET.

For the determination of the white-box model of the boost converter, state-space equations of the circuit are used. Considering the circuit in Figure 3, the inductor current i_L and the capacitor voltage v_c have been chosen as the state variables. When the period of the PWM signal is T_s and the duty cycle is d, the converter circuit can be examined in two states. In the first state $0 < t < \mathrm{d}T_s$, the Q_1 switch is off. So the current comes from the input stored as magnetic energy in the inductor L_1. In the second state $\mathrm{d}T_s < t < (1-d)T_S$, the Q_1 switch is on. So the stored current in the inductor is released by the diode D_1 to the capacitor C_1. Figure 3 shows the schematics of the two states of the circuit for state-space analysis.

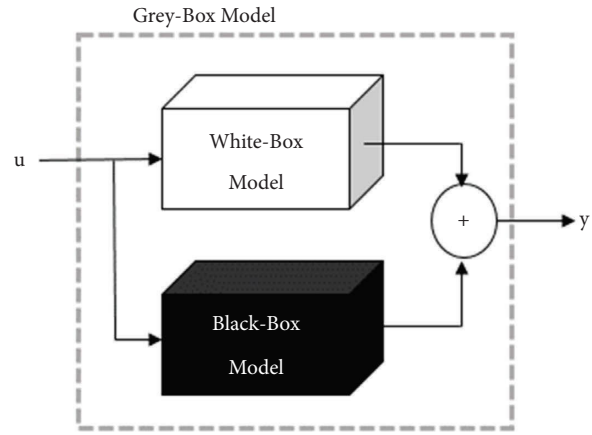

Figure 1: Proposed grey-box model.

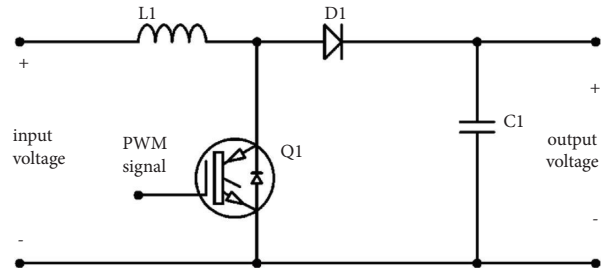

Figure 2: Basic single-stage boost converter circuit diagram.

For the on-state, $v_i = v_L$ and $i_C = -i_R$. Thus, $v_o = v_c$ and

$$\begin{aligned} \frac{\mathrm{d}i_L}{\mathrm{d}t} &= \frac{1}{L}v_i, \\ \frac{\mathrm{d}v_c}{\mathrm{d}t} &= -\frac{1}{\mathrm{RC}}v_c. \end{aligned} \tag{1}$$

So, for the on-state, the state equations and the output equations can be written as

$$\begin{aligned} \begin{bmatrix} \dot{i}_L \\ \dot{v}_c \end{bmatrix} &= \begin{bmatrix} 0 & 0 \\ 0 & -\dfrac{1}{\mathrm{RC}} \end{bmatrix} \begin{bmatrix} i_L \\ v_c \end{bmatrix} + \begin{bmatrix} \dfrac{1}{L} \\ 0 \end{bmatrix} [v_i], \\ v_o &= \begin{bmatrix} 0 & 1 \end{bmatrix} \begin{bmatrix} i_L \\ v_c \end{bmatrix}. \end{aligned} \tag{2}$$

For the off-state, $v_i = v_L + v_c$ and $i_c = i_L - i_R$. Thus, $v_o = v_c$ and

$$\begin{aligned} \frac{\mathrm{d}i_L}{\mathrm{d}t} &= \frac{1}{L}v_i - \frac{1}{L}v_c, \\ \frac{\mathrm{d}v_c}{\mathrm{d}t} &= \frac{1}{C}i_L - \frac{1}{\mathrm{RC}}v_c. \end{aligned} \tag{3}$$

So, for the off-state, the state equations and the output equations can be written as

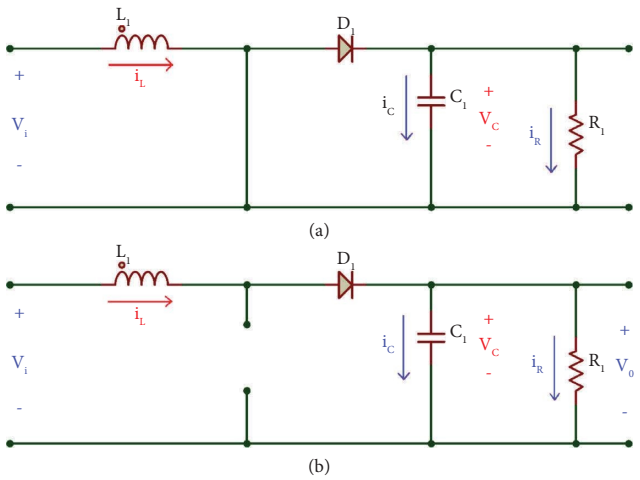

Figure 3: The state schematics of the boost converter circuit: (a) the on-state of the boost converter circuit ($0 < t < dT_s$) and (b) the off-state of the boost converter circuit ($dT_s < t < (1-d)T_S$).

$$\begin{bmatrix} \dot{i}_L \\ \dot{v}_c \end{bmatrix} = \begin{bmatrix} 0 & -\frac{1}{L} \\ \frac{1}{C} & -\frac{1}{\mathrm{RC}} \end{bmatrix} \begin{bmatrix} i_L \\ v_c \end{bmatrix} + \begin{bmatrix} \frac{1}{L} \\ 0 \end{bmatrix} [v_i], \quad v_o = \begin{bmatrix} 0 & 1 \end{bmatrix} \begin{bmatrix} i_L \\ v_c \end{bmatrix}. \tag{4}$$

From equations (2) and (4), the averaged large-signal model of the boost converter for $0 < t < T_s$ can be written as shown in the following equation. These equations are used as a state-space model for the boost converter circuit.

$$\begin{bmatrix} \dot{i}_L \\ \dot{v}_c \end{bmatrix} = \begin{bmatrix} 0 & -\frac{(1-d)}{L} \\ \frac{1-d}{C} & -\frac{1}{RC} \end{bmatrix} \begin{bmatrix} i_L \\ v_c \end{bmatrix} + \begin{bmatrix} \frac{1}{L} \\ 0 \end{bmatrix} [v_i], \quad v_o = \begin{bmatrix} 0 & 1 \end{bmatrix} \begin{bmatrix} i_L \\ v_c \end{bmatrix}. \tag{5}$$

The state-space equations of the boost converter circuit are embedded in a state-space block in MATLAB/Simulink for the simulation of the white-box part of the module. Figure 4 shows the state-space block and the block parameters for the white-box model of the DC/DC converter. As mentioned above, the state-space model contains the state variables (i_L and v_C) and their derivatives ($\dot{i}_L$ and $\dot{v}_c$) together. The state variables are related to circuit output resistance, inductor, and capacitor. The duty cycle variable (d) is added to the module to express the switching effect of the boost converter circuit. v_i is described as the model input signal and v_o is described as the model output signal. Matrix A is the coefficient of the effect of the state variables on derivatives of the state variables, matrix B is the coefficient of the effect of the input variable on derivatives of the state variables, and matrix C is the coefficient of the effect of the state variables on output. In this case, the matrix D, the coefficient of the effect of the input variable to the output variable is equal to zero.

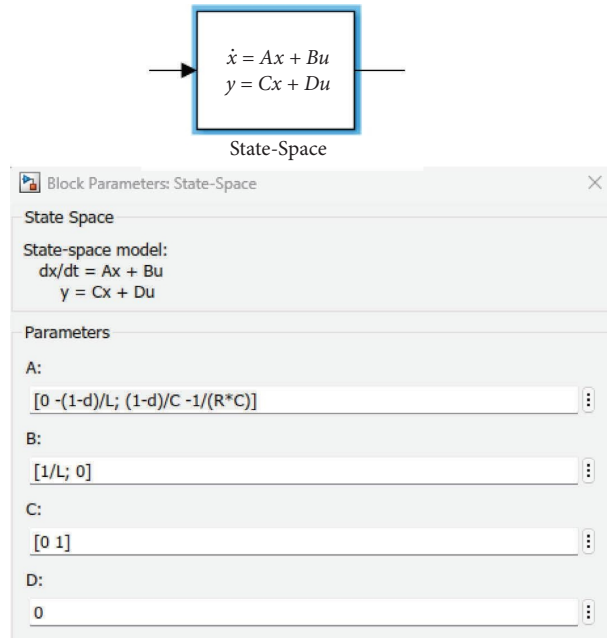

Figure 4: Simulink state-space block and the block parameters.

2.1.2. The Black-Box Model. In the literature, the black-box identification method is generally used to describe the effects of dynamic system parameters, which are difficult to express mathematically on the system output signal. In DC/DC converters, the magnetic field created by the coil changes with the coil temperature. The inductor voltage is related to the magnetic field created on the coil. Inductor voltage is an important factor affecting the output voltage of the circuit. Therefore, it is difficult to express the effect of electromagnetic field changes occurring in the inductor on the output voltage with mathematical equations. However, the voltage stress on switches, diodes, and other components is also difficult to model by mathematical equations. For this reason, in this study, the black-box identification method is used to model dynamic voltage changes that are difficult to express mathematically.

For black-box identification, a feed-forward back-propagation type ANN is created in MATLAB/Simulink. The created ANN has one input layer, one output layer, and one hidden layer. The hidden layer of the network contains five neurons. The number of neurons in the hidden layer is defined by using a pruning algorithm. The ANN structure is given in Figure 5. The neurons have tangent-sigmoid activation function inside. Every neuron has weight factors and biases.

The created ANN has two inputs and one output. The inputs of the ANN are the PV panel output voltage and duty cycle of the DC/DC converter. The output of the ANN is the DC/DC converter output voltage.

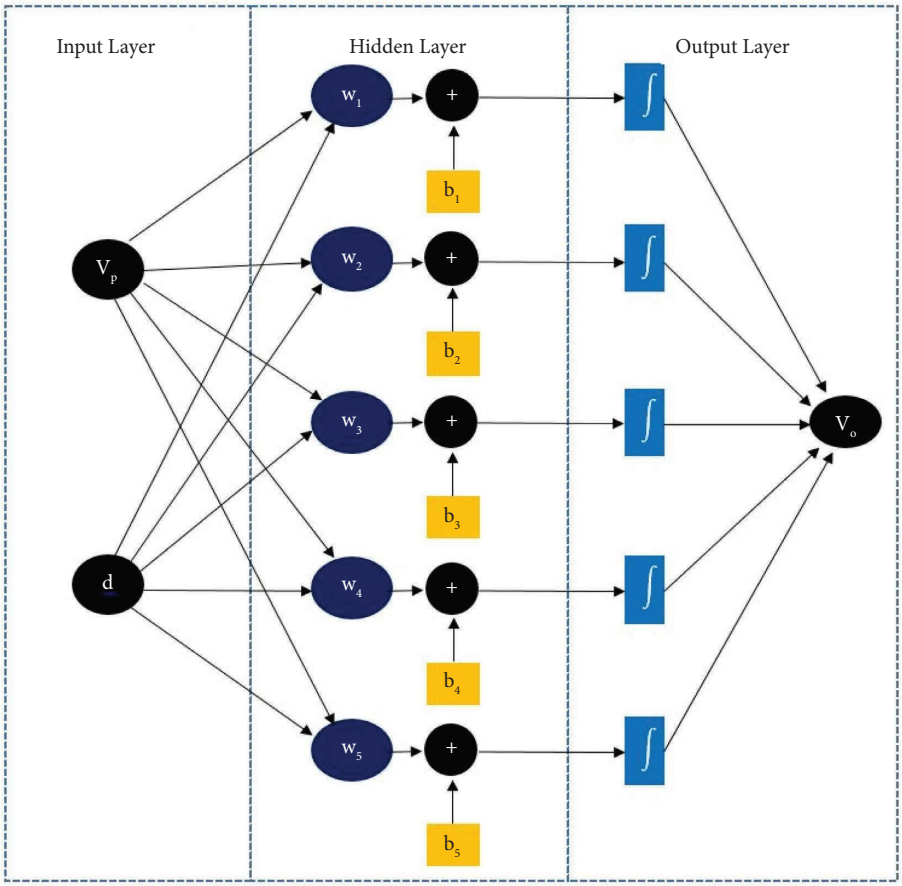

Figure 5: Artificial neural network structure.

(1) Training of the ANN. The ANN training data are obtained from a boost converter circuit that is connected to a 10 kW PV energy system. The PV energy system consists of 3 parallel PV panel strings, each of them consisting of 14 PV panels in series. The PV energy system is located in Izmir, Turkey. The panel tilt angle is 45 degrees and the panel direction is directed to the south. Figure 6 shows the electrical characteristics of the PV energy system. The maximum power output of one PV panel is 243 watts. The open circuit voltage of one panel is 38.3 volts. The short circuit current of one panel is 8.81 amperes. The maximum power point voltage of one panel is 30.2 volts. The maximum power point current of one PV panel is 8.06 amperes.

The DC/DC boost converter circuit in Figure 7 is used for training the ANN. The DC/DC boost converter circuit consists of an 80 mH inductor denoted as L, a 1200 V 100 A IGBT denoted as Q, two 1200 V fast switching diodes in series denoted as D, a 100 μF output capacitor denoted as C, a 0.1 μF capacitor as a snubber capacitor denoted as C_s, and a snubber resistor denoted as R_s. The component details are given in Table 1. The IGBT in the circuit is triggered with an external driver circuit with a switching frequency of 10 kHz. The switching signal is generated by a PIC microcontroller. The driver circuit allows the duty cycle value to be changed between 1% and 95%. To prevent the circuit from being damaged due to high current, the duty time upper limit is limited to 95%.

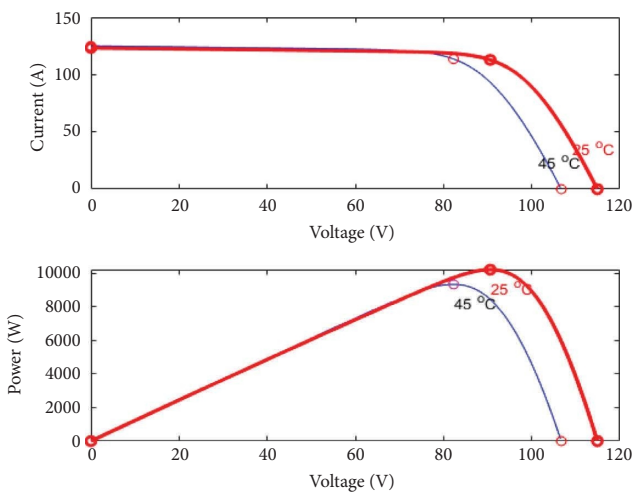

Figure 6: Proposed PV energy system voltage-current and voltage-power characteristics (PV panel properties: $P_{mpp} = 243$ W, $V_{oc} = 38.3$ V, $I_{sc} = 8.81$ A, $V_{mpp} = 30.2$ V, and $I_{mpp} = 8.06$ A).

The ANN training data have two inputs and one output. The inputs are V_i (converter input voltage) and d (duty cycle of the PWM signal). The output is V_o (the converter output voltage). For the compilation of training data, boost converter input voltage (as PV panel output voltage) and boost converter

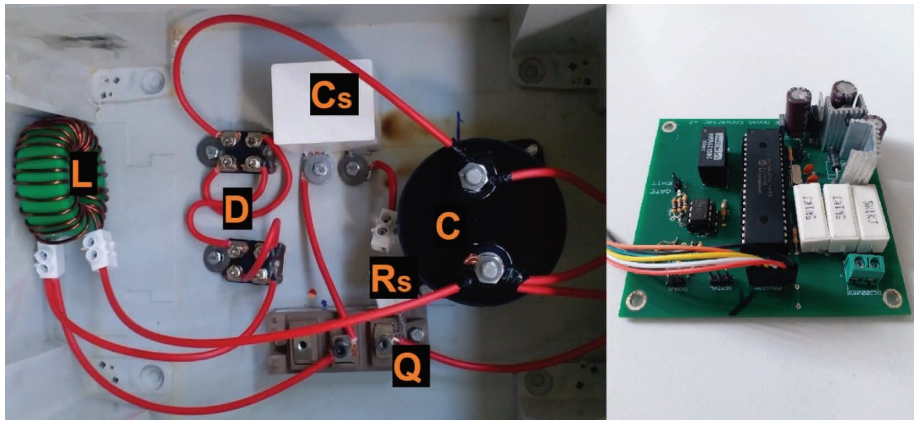

Figure 7: DC/DC converter circuit and the external driver circuit used in experiments.

Table 1: Details of the components in the boost converter circuit.

Component	Value
Inductor (L)	80 mH
IGBT (Q)	1200 V 100 A
Diode (D)	1200 V fast switching diodes
Output capacitor (C)	100 μF
Snubber capacitor (C_s)	0.1 μF
Snubber resistor (R_s)	50 kΩ

output voltage values are measured when the solar irradiance value increases from 100 W/m^2 to 1000 W/m^2 by 100 W/m^2 step. The duty cycle value is changed from 20% to 80% by 10% step increases for each 100 W/m^2 solar irradiance period. Figure 8 represents the three-dimensional training dataset obtained from the real boost converter circuit.

For a better understanding of the training data, Figure 9 displays a transection of the training data representing input voltage ranging from 107 V to 109 V and duty cycle ranging from 60% to 70%. The training data comprise 40 transections, as illustrated in Figure 9.

2.1.3. The Grey-Box Model. The proposed grey-box model Simulink diagram is shown in Figure 10. There, input signals interact with the white-box part and the black-box part together (since there is no input for the duty cycle for the state-space block, duty cycle changes are made by an external.m file during simulations.). Then, these two signals are averaged. The advantage of averaging the white-box model and black-box model outputs is that the system dynamics can be added to the model output at a sufficient level. The general goal of averaging two signals is as follows: The white-box model system does not include some system dynamics as explained in the previous sections. The black-box model, on the other hand, may contain more system dynamics than necessary because the data in the identification process made with the artificial neural network are insufficient in some cases. In the grey-box model, which is designed as a model in which the outputs of two models are averaged, the deficiencies of the white-box model output are completed, and it is also aimed to prevent excessive dynamic behavior effects on the system output.

The model is simulated by connecting to a PV array block that simulates PV panels, and measurements of the input-output signals have been taken. The PV array block in the simulation consists of 14 PV panels in series and 3 PV panels in parallel strings. Figure 11 shows the Simulink diagram of the proposed grey-box DC/DC converter model with the PV energy system.

The proposed grey-box model of the boost converter is shown in a subsystem. Inside the subsystem, a white-box part of the model and a black-box part of the model work in parallel. The PV panel I–V block is a scope for the PV panel output current, PV panel output voltage, and solar irradiance. The panel temperature is simulated as 25 centigrade degrees. An output capacitor is connected in parallel to the PV panel block to dampen the output voltage spikes.

3. Simulation Results

In simulation studies, while the solar radiation value is 800 W/m^2, the duty cycle is changed between 20% and 90% ($d = 0.2$ to $d = 0.9$). In these changes, the waveforms of the white-box model, black-box model, and grey-box model outputs are examined. Transient state responses and steady-state responses of the model outputs are observed. The reasons for the fluctuations in transient responses are tried to be explained.

Figure 12 presents the output of the white-box model simulation. When examining the white-box model output, fluctuations in the transient response become apparent. These temporary fluctuations start from a high value and gradually fade away and disappear. The frequency of these fluctuations is high, ranging from 20% to 50% of the duty cycle. The frequency of fluctuations in the transient response appears to be lower when the duty cycle is in the range of 60%–90%. It is thought that these fluctuations occur as a result of the capacitor and the inductor in the model entering into resonance. Another reason for the fluctuations may be the absence of damping resistive elements or snubber capacitances modeled in the white-box model. Therefore, the imprecision of the output transient response at lower duty cycles can be attributed to these omissions.

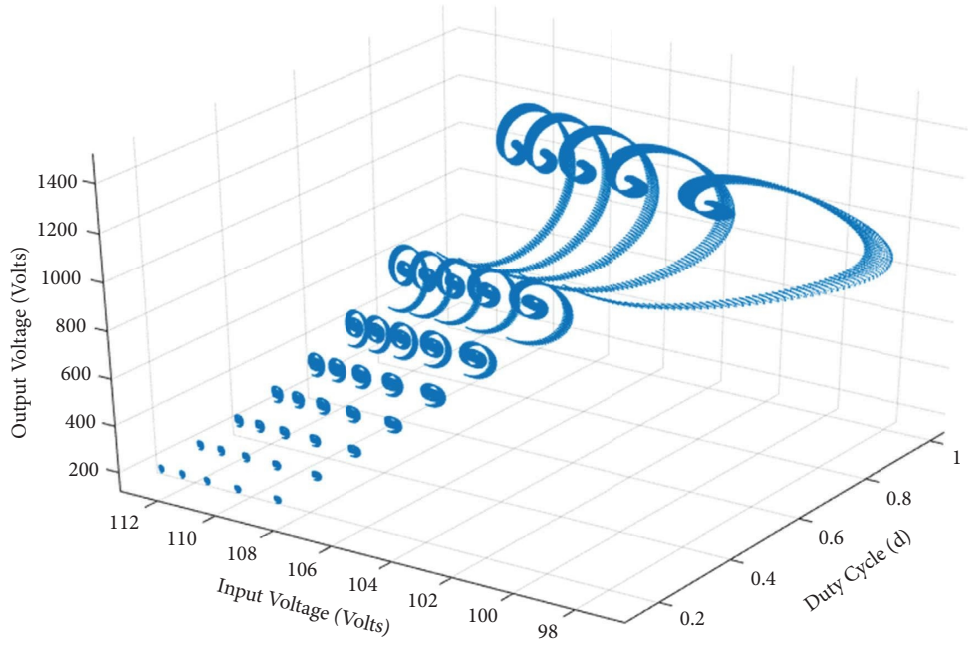

Figure 8: Training data of ANN for $i_r = 500\ \mathrm{W/m^2}$: correspondingly, boost converter input voltage, duty cycle, and boost converter output voltage.

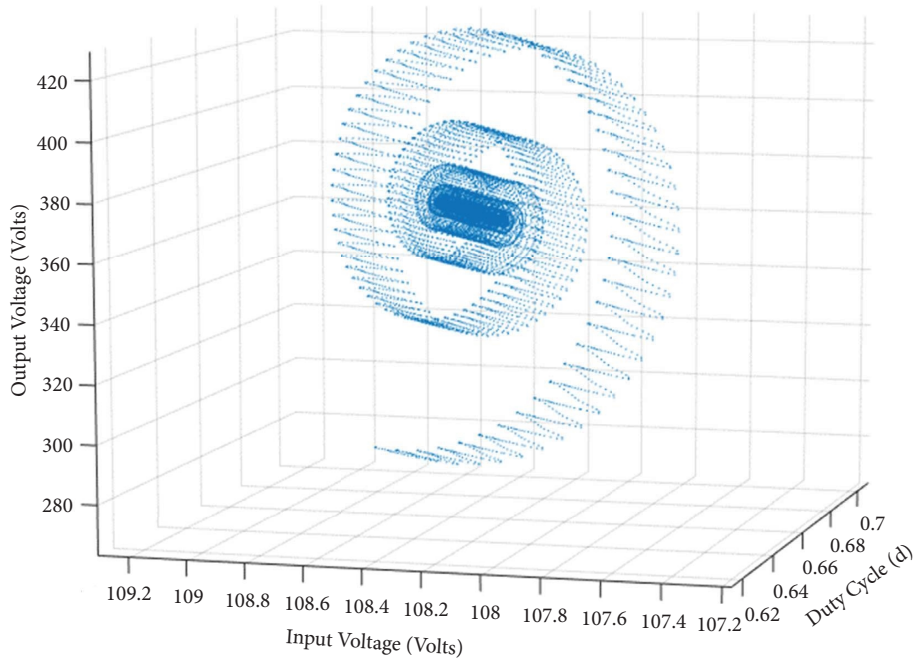

Figure 9: A transection of the training dataset corresponding to input voltage from 107 V to 109 V and duty cycle from 60% to 70%.

Figure 13 depicts the output of the black-box model under the same conditions. Upon examination of the black-box model output, it becomes apparent that the artificial neural network primarily focuses on the steady state of the system output, especially when the duty cycle is between 20% and 60%. Conversely, when the duty cycle falls within the range of 70%–90%, the artificial neural network predicts transient responses more accurately. This behavior of the artificial neural network can serve as a factor in reducing the controller response time for designs aiming to stabilize the output voltage. However, it is not deemed suitable for standalone use in modeling, as it provides fewer transient responses than necessary.

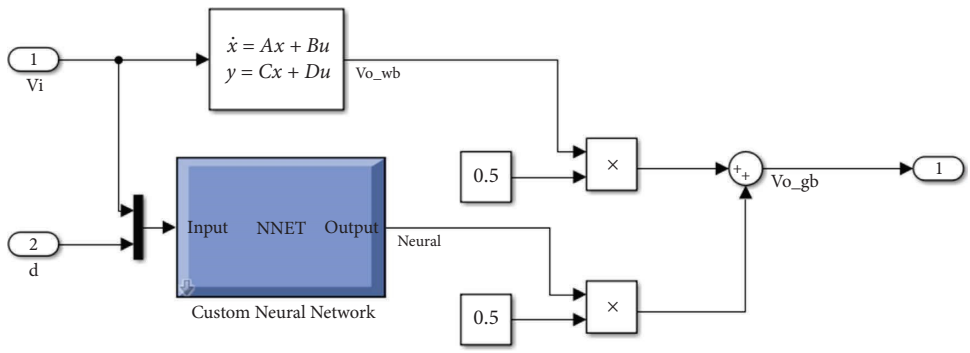

Figure 10: The proposed grey-box model of the boost converter.

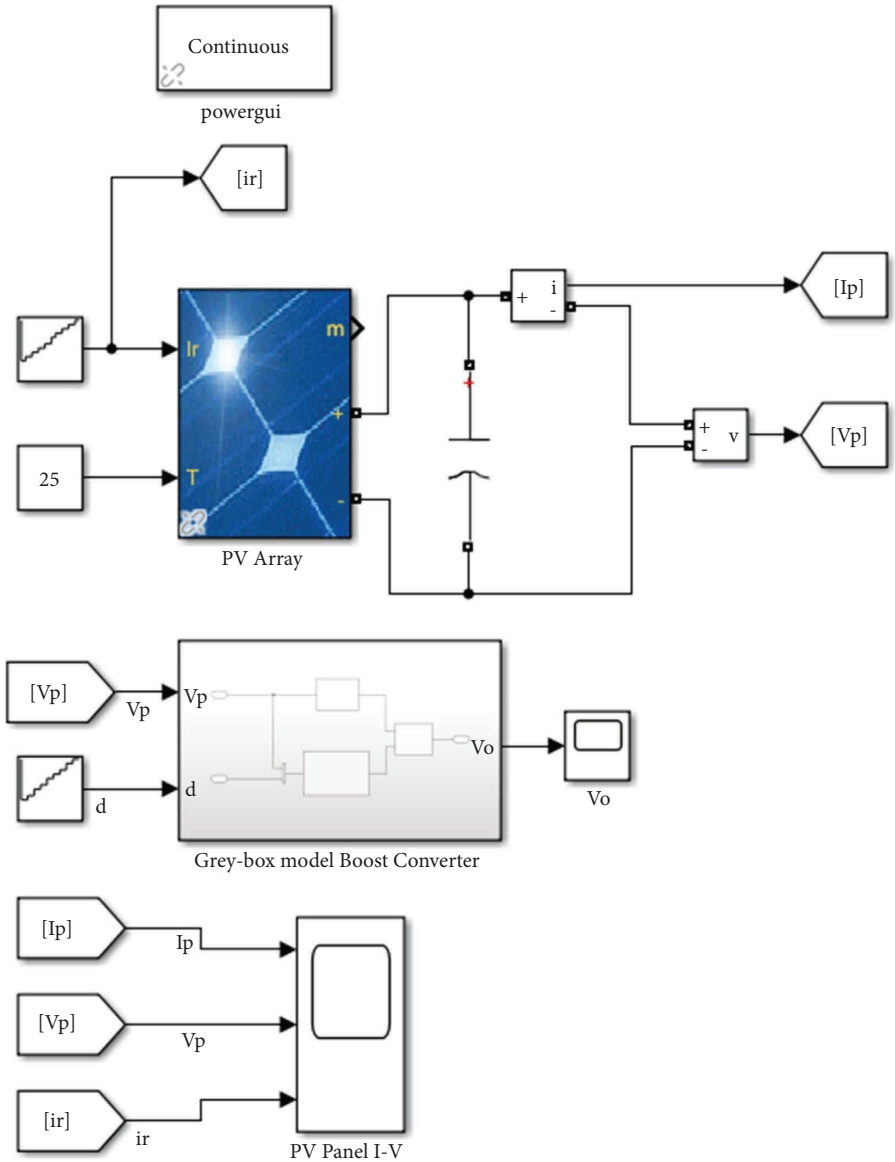

Figure 11: Simulink diagram of the proposed grey-box model (PV panel properties: $P_{mpp} = 243$ W, $V_{oc} = 38.3$ V, $I_{sc} = 8.81$ A, $V_{mpp} = 30.2$ V, and $I_{mpp} = 8.06$ A).

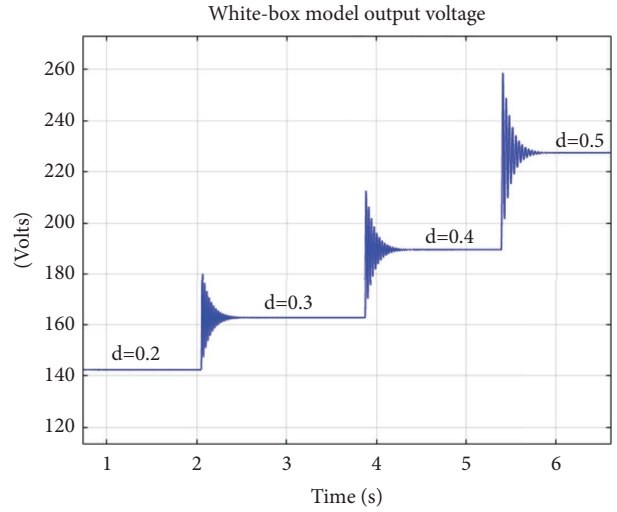

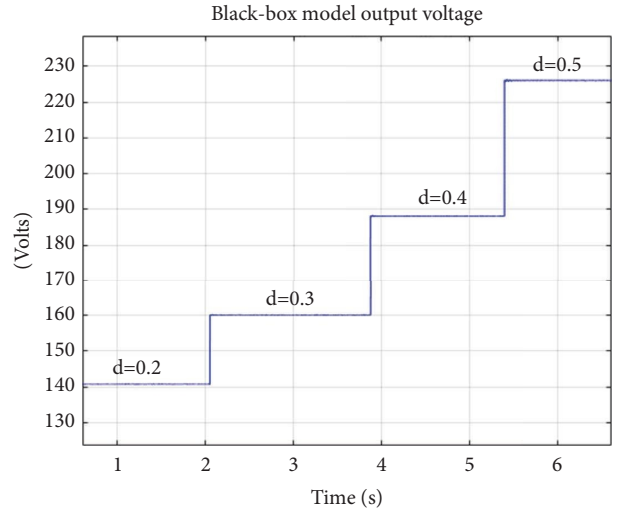

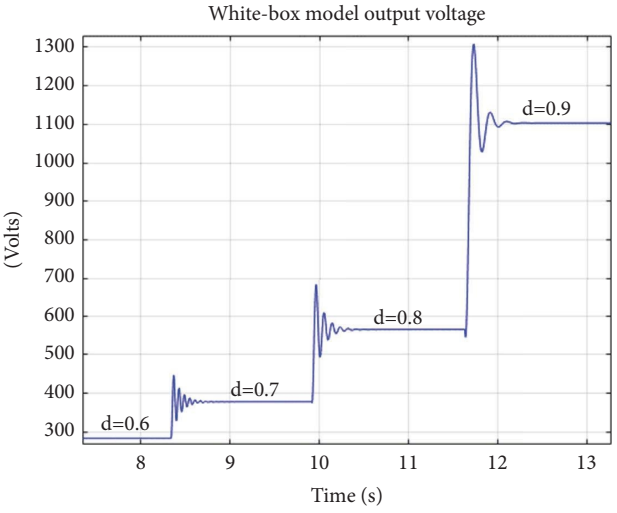

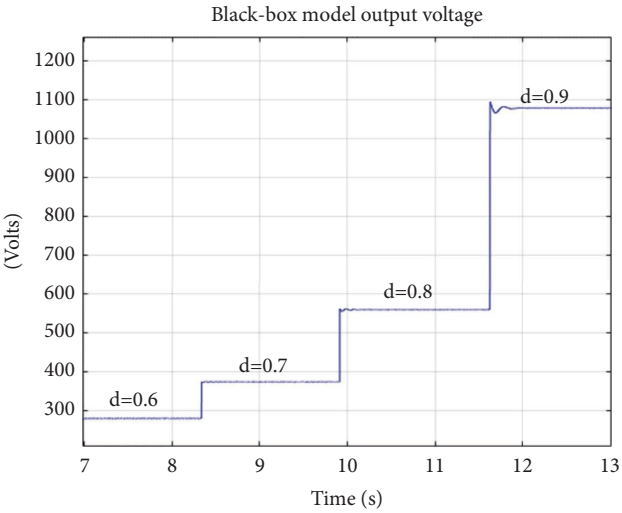

FIGURE 12: Steady-state model output corresponding to duty cycle from 0.2 to 0.9 at 800 W/m^2 solar irradiance.

FIGURE 13: Black-box model output voltage corresponding to duty cycle from 0.2 to 0.9 at 800 W/m^2 solar irradiance.

Figure 14 illustrates the output of the grey-box model, aiming to amalgamate the advantages of both the white-box and black-box models. Upon examination of the grey-box model output, it is observed that transient state responses are present in the signal, although not as pronounced as in the white-box model. However, steady-state responses are established more rapidly compared to the white-box model. The proposed grey-box model addresses the issue of the black-box model's deficiency in transient response, resulting in a more realistic representation of step-up DC/DC converters.

4. Experimental Results

In this section, the proposed grey-box model of the DC/DC boost converter simulation results and experimental results are compared. A 10 kW PV array on the top roof of the Solar Energy Institute, Ege University, Turkey, is used for the experimental study. The single-stage DC/DC boost converter circuit in Figure 7 is used for the experiments. A time period in which solar radiation is 800 W/m^2 during the day is chosen for the experiments. The duty cycle is changed from 20% to 90% for boosting the output voltage.

4.1. Calculation of the Correlation Coefficient. The correlation coefficient between model output signals and the real boost converter output signal is calculated by using the method described as follows.

The correlation coefficient between two random variables quantifies the strength of their linear relationship [21]. When each variable comprises N scalar observations, the Pearson correlation coefficient is defined as follows:

$$\rho(A,B) = \frac{1}{N-1}\sum_{i=1}^{N}\left(\frac{A_i-\mu_A}{\sigma_A}\right)\left(\frac{B_i-\mu_B}{\sigma_B}\right), \quad (6)$$

where μ_A and σ_A are the mean and standard deviation of A, respectively, and μ_B and σ_B are the mean and standard deviation of B. Alternatively, the correlation coefficient can be expressed in terms of the covariance of A and B as

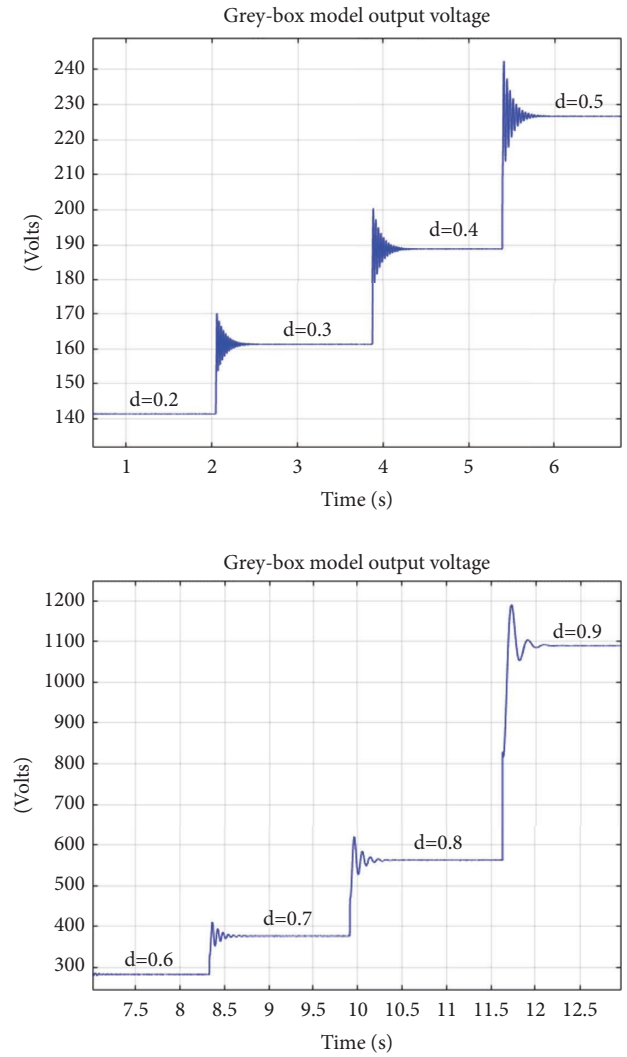

Figure 14: Grey-box model output voltage corresponding to duty cycle from 0.2 to 0.9 at 800 W/m^2 solar irradiance.

$$\sigma(A,B) = \frac{\operatorname{cov}(A,B)}{\sigma_A \sigma_B}. \tag{7}$$

The correlation coefficient matrix for two random variables represents a matrix containing correlation coefficients calculated for each possible pair of variables.

$$R = \begin{pmatrix} \rho(A,A) & \rho(A,B) \\ \rho(B,A) & \rho(B,B) \end{pmatrix}. \tag{8}$$

As A and B are inherently correlated with themselves, the diagonal entries of the correlation coefficient matrix are always 1. Therefore, the correlation coefficient R can be represented by using the following equation:

$$R = \begin{pmatrix} 1 & \rho(A,B) \\ \rho(B,A) & 1 \end{pmatrix}. \tag{9}$$

4.2. Model Comparisons. First, the existing white-box model output is compared with the output signal of the real boost converter circuit. As is seen in Figure 15, the white-box model output has many fluctuations in the transient response. However, the experimental output does not have as many fluctuations as the white-box model. The correlation between the white-box model output and the experimental output is 0.9360. On the other hand, the steady-state response of the white-box model is nearly the same as the original output signal. So, it is understood that the white-box model is not suitable for modeling a boost converter alone.

Then, the black-box model of the boost converter circuit output is compared with the experimental results. Figure 16 shows the transient responses of the real boost converter output signal and black-box model output. According to the scope view, the black-box model responds quicker than the white-box model. It makes it more suitable to use the black-box model than the white-box model for controller applications. However, the black-box model lacks transient responses. The correlation between the black-box model output and the experimental output is 0.9612. So the black-box model is considered to need to be improved.

Then, the proposed grey-box model is compared with the experimental data. The results of the experiments showed that the proposed grey-box model (the white-box model with ANN black-box identification) correlates with the original output signal better than the existing white-box model and black-box model. Figure 17 illustrates the real boost converter output signal and grey-box model output corresponding to the duty cycle from 0.2 to 0.9 at 800 W/m^2 solar irradiance. It is found that the correlation between the original boost converter output voltage value and the proposed grey-box model output is 0.9690. The proposed grey-box model can be used for both controller design and transient response analysis of DC/DC boost converter circuits.

It is thought that the reason for the deviation in transient time responses at low duty cycle values in the models is due to the fact that damping elements are not defined in the white-box model. However, since the white-box model is partially used in the grey-box model, it can be interpreted that deviations occur at low duty cycle values in the grey-box model. However, in the grey-box model, it is observed that this handicap is reduced by half, as the white-box model output is combined with the black-box model.

4.3. Experiments under Load Variations. The featured models have been tested over a wide range of resistive loads from 100 ohms to 1 M ohms. The correlation between the outputs of the proposed model and the output of the real system was examined. The results of the experiments conducted under a wide variety of loads are shown in Table 2. At each load value, 8 experiments were carried out by changing the duty cycle in the range of 20%–80% with increments of 10%. The correlation coefficient was calculated for each of these experiments, and the average value of the calculated correlation coefficients was written in the section of the relevant model in the table.

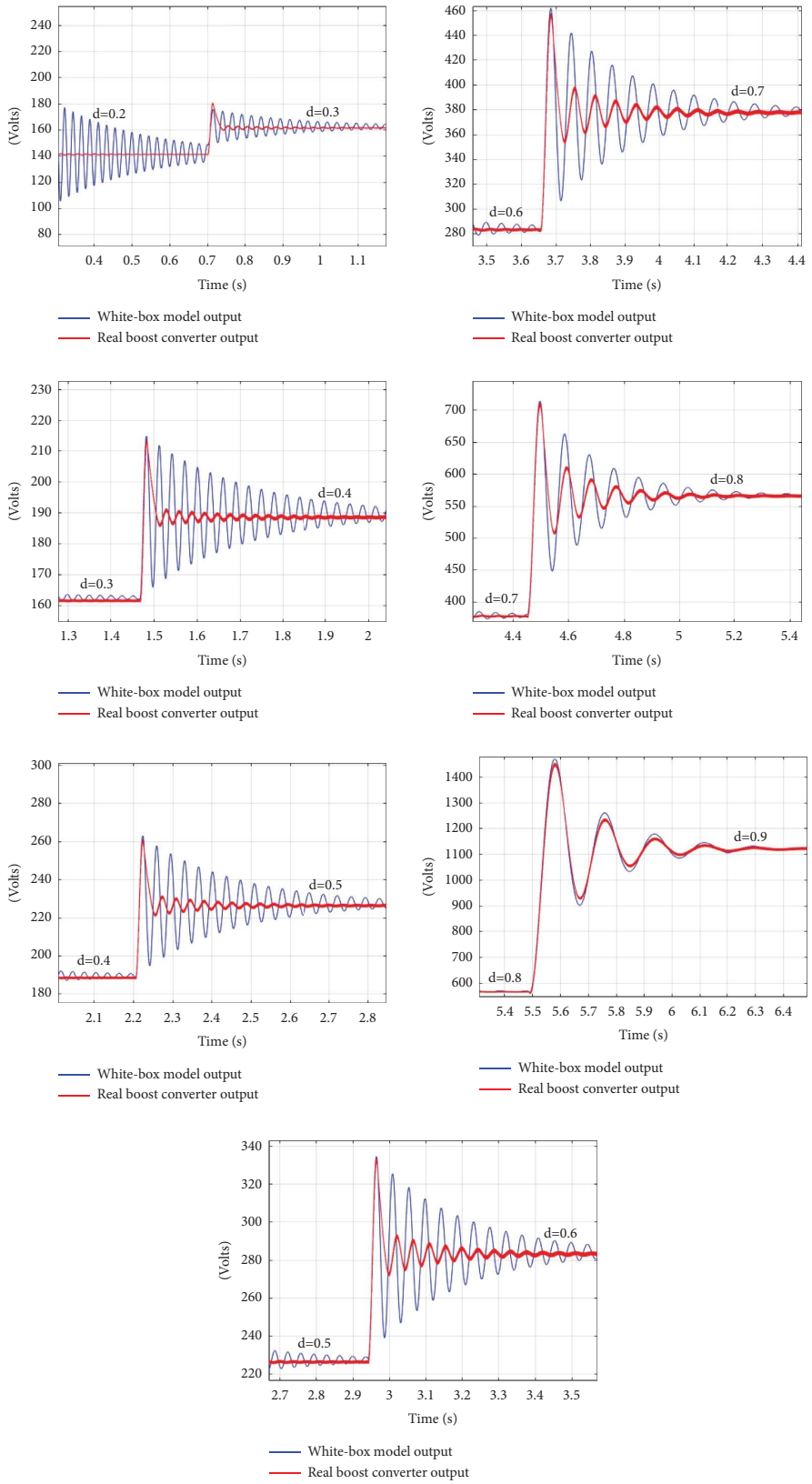

FIGURE 15: Transient responses of the real boost converter output signal and white-box model output corresponding to duty cycle from 0.2 to 0.9 at 800 W/m^2 solar irradiance (output resistance $R = 1150\,\Omega$).

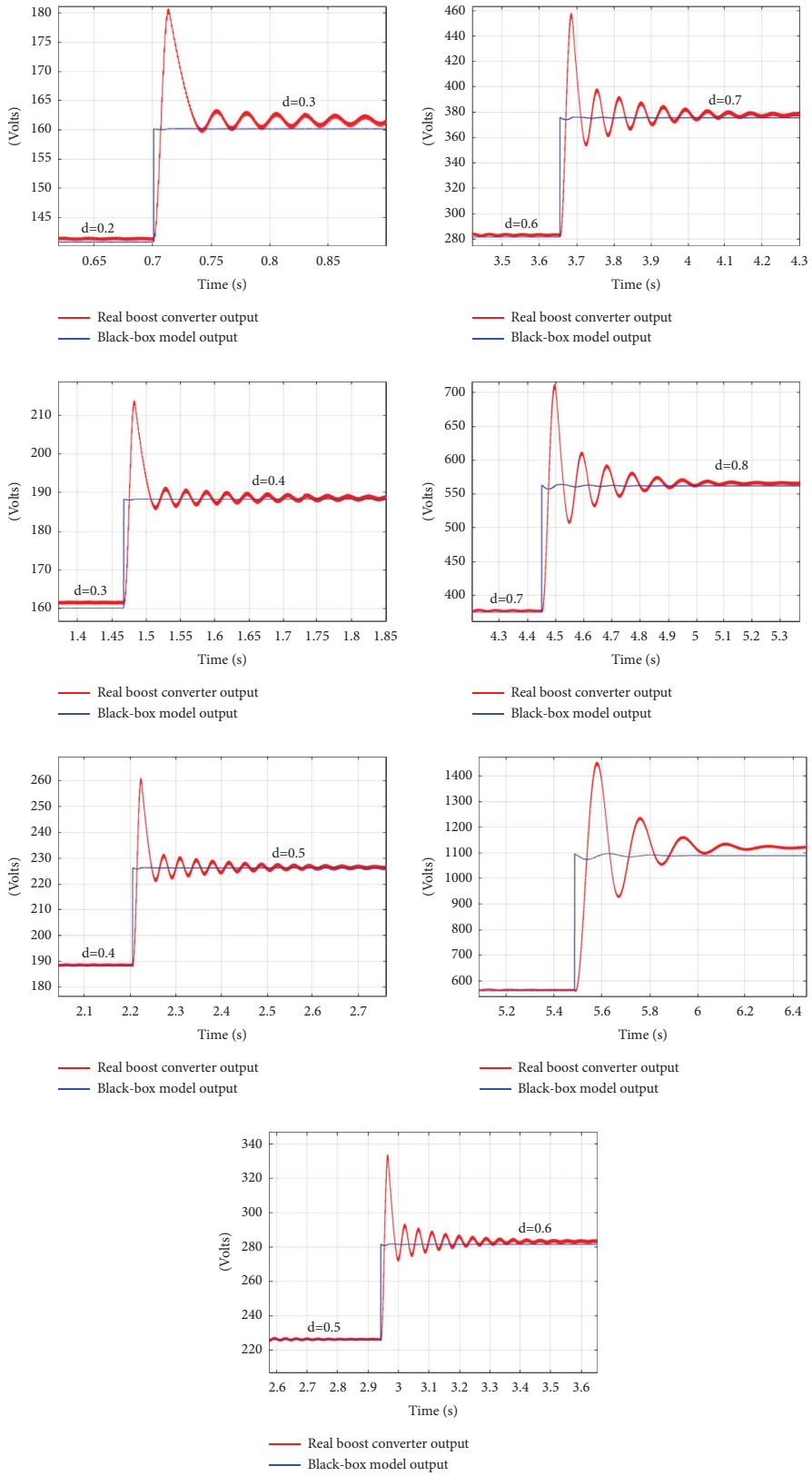

FIGURE 16: Transient responses of the real boost converter output signal and black-box model output corresponding to duty cycle from 0.2 to 0.9 at 800 W/m^2 solar irradiance (output resistance $R = 1150\,\Omega$).

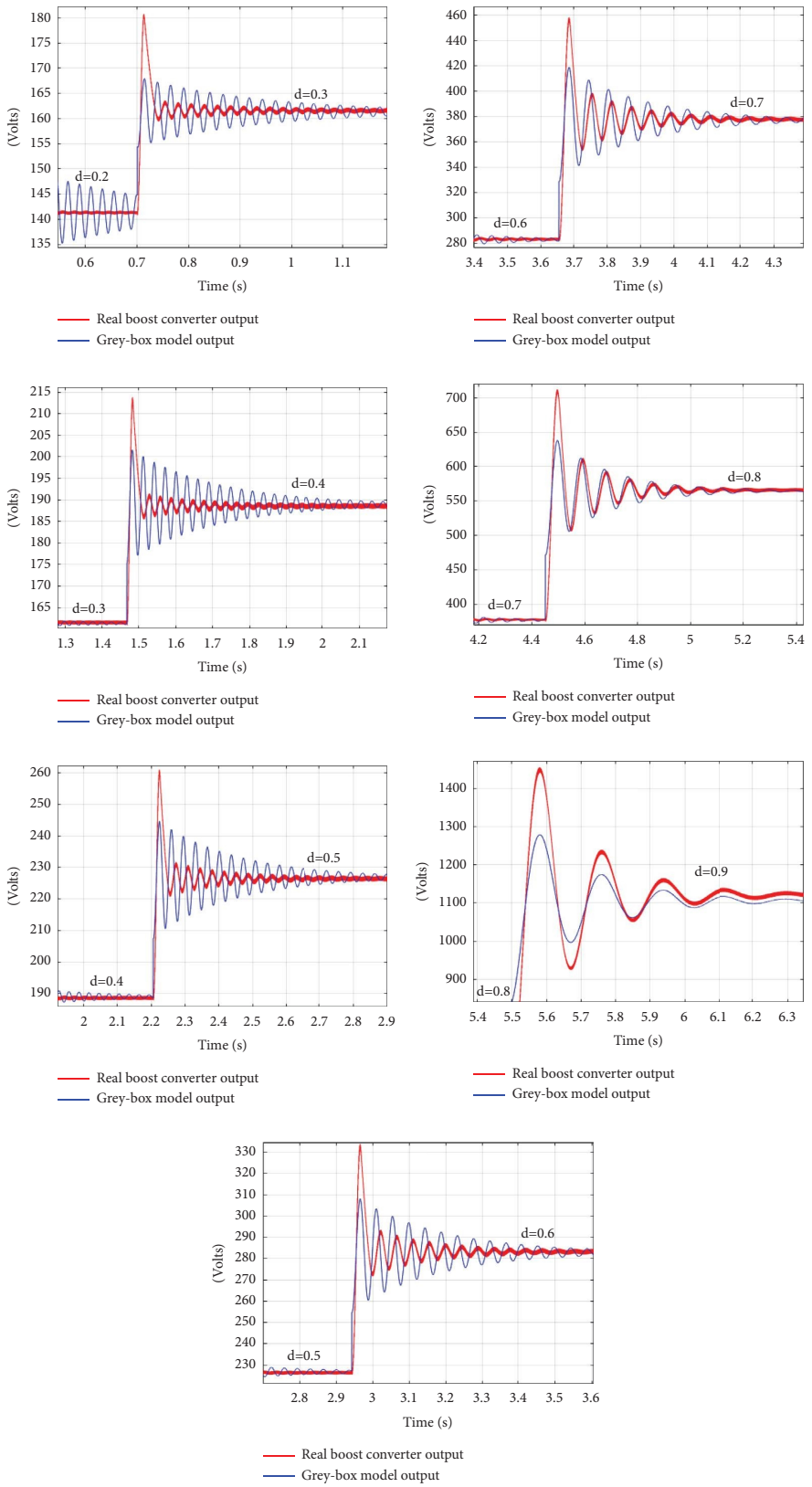

FIGURE 17: Transient responses of real boost converter output signal and grey-box model output corresponding to duty cycle from 0.2 to 0.9 at 800 W/m^2 solar irradiance (output resistance $R = 1150\,\Omega$).

Table 2: Correlation coefficients of the proposed models corresponding to load resistance.

Load	Correlation coefficient		
	White-box model	Black-box model	Grey-box model
100 Ω	0.969607374871639	0.989513638531563	0.989820560464109
200 Ω	0.976144494547240	0.991640393050001	0.993413906368015
300 Ω	0.976923513467295	0.990436320971092	0.993590316644113
400 Ω	0.979988267054458	0.989421560287630	0.993837996469483
500 Ω	0.980225900502161	0.988866958508408	0.993865075783872
600 Ω	0.985603416035943	0.989670275878091	0.994144100656739
700 Ω	0.982795930071293	0.986884751559852	0.993201940018121
800 Ω	0.984517235328024	0.987159320329735	0.992496091425469
900 Ω	0.982673910426754	0.988889783662086	0.993452111138890
1 kΩ	0.979762754682253	0.986772163427075	0.991985164520238
2 kΩ	0.976144494547240	0.991640393050001	0.993413906368015
3 kΩ	0.976923513467295	0.990436320971092	0.993590316644113
4 kΩ	0.979988267054458	0.989421560287630	0.993837996469483
5 kΩ	0.980225900502161	0.988866958508408	0.993865075783872
6 kΩ	0.985603416035943	0.989670275878091	0.994144100656739
7 kΩ	0.982795930071293	0.986884751559852	0.993201940018121
8 kΩ	0.984517235328024	0.987159320329735	0.992496091425469
9 kΩ	0.982673910426754	0.988889783662086	0.993452111138890
10 kΩ	0.935970454110177	0.961261382638612	0.963262087672671
20 kΩ	0.931870554390938	0.963208688647779	0.965073476115451
30 kΩ	0.933618975230007	0.959623222565440	0.961791180543948
40 kΩ	0.933903318154406	0.959545572674599	0.961225377879551
50 kΩ	0.913986342412283	0.949099664989821	0.950941023597757
60 kΩ	0.930819295880845	0.957568658115150	0.958862100443451
70 kΩ	0.930682875491503	0.955620053912268	0.957565076893362
80 kΩ	0.924463965754733	0.955476590411907	0.956782645035189
90 kΩ	0.932454024167612	0.959497120248109	0.960276549391506
100 kΩ	0.934523015669254	0.958883606912570	0.959847019029370
200 kΩ	0.926376070445581	0.959697268346821	0.960287822022982
300 kΩ	0.934618234112205	0.958547227511676	0.959703720185535
400 kΩ	0.924483253918741	0.956441961509381	0.957258335268235
500 kΩ	0.918083893513768	0.954893996522147	0.956127236637524
600 kΩ	0.922747183436913	0.954612204426463	0.955873694057610
700 kΩ	0.932109903206404	0.958829830993813	0.959931624512020
800 kΩ	0.912661691575812	0.947996746439804	0.949092672243520
900 kΩ	0.920549605992836	0.949959031814387	0.951848302572760
1 MΩ	0.928352443784171	0.958162827359424	0.958908262966600

When Table 2 is examined, it appears that for the load between 100 ohms and 1 kohm, the models are similarly correlated with the results of the real system by approximately 99%. However, it is observed that the accuracy of the white-box model output gradually decreases when the load resistance is larger than 1 kohm. It is observed that when the load resistance reaches levels of several hundred kilo-ohms, the correlation coefficient of the white-box model output drops to 91%. Within the same range, the black-box model correlates with actual results around 95%, while this value for the grey-box model is 96%. The change of the correlation coefficient corresponding to load resistance is given in Figure 18.

As a result of the experiments and simulation studies, the correlation of the white-box model output with the real experiment outputs was found to be 0.9532, that of the black-box model to be 0.9625, and that of the grey-box model to be 0.9752. While the black-box model outperformed the white-box model, the grey-box model demonstrated an even higher level of performance.

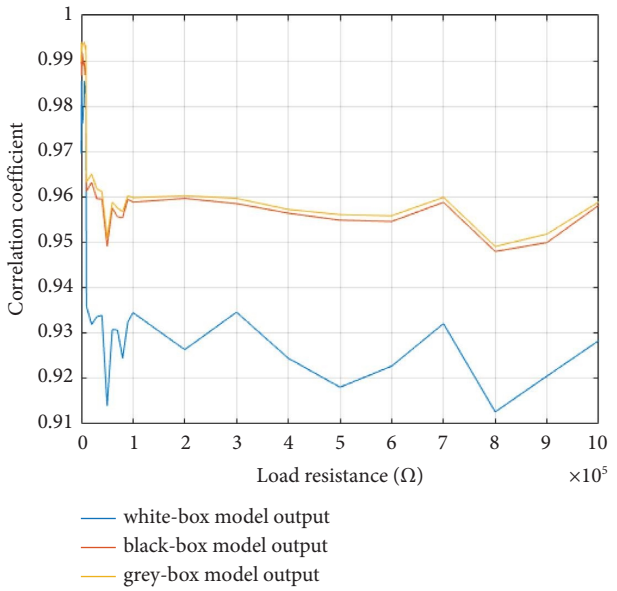

FIGURE 18: Change of the correlation coefficient corresponding to load resistance.

5. Conclusion

This paper proposes a grey-box model for a better understanding of the input-output behavior of DC/DC boost converters. The physical characteristics of the circuit are modeled by the state-space equations, and a nonlinear black-box identification is made by an ANN for circuit dynamics.

Results of the simulations and experimental studies showed that the average correlation of the proposed grey-box model output with the real experiment outputs is 97.52%.

The proposed grey-box model can be used for transient output voltage analysis. It can also be used for faster controller designs for output voltage stabilization of DC/DC converter circuits.

In future studies, novel controller designs can be proposed by using the grey-box boost converter model to speed up the control operations in DC/DC boost converter circuits. Thus, it is aimed for PV renewable energy systems to react faster and therefore operate more efficiently when environmental conditions change.

Data Availability

The data used to support the findings of the study are available from the corresponding author upon request.

Conflicts of Interest

The authors declare that they have no conflicts of interest.

Acknowledgments

The authors sincerely thank Ege University Solar Energy Institute for the use of the solar energy system for obtaining training data. The authors also thank TUBITAK (Scientific and Technological Research Council of Turkey) for its support for the publication of the article as open access. This study was funded by TUBITAK (Scientific and Technological Research Council of Turkey) project number 2190143.

References

[1] Z. Zhao, H. Hu, Z. He et al., "A transient-modeling-based grey-box method for online monitoring of DC-link capacitors," *IEEE Transactions on Power Electronics*, vol. 38, no. 11, pp. 14547–14562, 2023.

[2] J. Ungerland, N. Poshiya, W. Biener, and H. Lens, "A voltage sensitivity based equivalent for active distribution networks containing grid forming converters," *IEEE Transactions on Smart Grid*, vol. 14, no. 4, pp. 2825–2836, 2023.

[3] V. Roosta, S. M. Ghamari, H. Mollaee, and M. H. Zarif, "A novel adaptive neuro linear quadratic regulator (ANLQR) controller design on DC-DC buck converter," *IET Renewable Power Generation*, vol. 17, no. 5, pp. 1242–1254, 2023.

[4] M. Rosati, "A data-based modelling approach for a vented oscillating water column wave energy converter," in *Trends in Renewable Energies Offshore- Proceedings of the 5th International Conference on Renewable Energies Offshore, RENEW 2022*, crc press, Boca Raton, FL, USA, 2023.

[5] C. Wang, T. G. Zsurzsan, and Z. Zhang, "Genetic algorithm assisted parametric design of splitting inductance in high frequency GaN-based dual active bridge converter," *IEEE Transactions on Industrial Electronics*, vol. 70, no. 1, pp. 522–531, 2023.

[6] Y. Liu, Y. Xue, S. Huang, G. Xue, and Q. Jing, "Dynamic model identification of ships and wave energy converters based on semi-conjugate linear regression and noisy input Gaussian process," *Journal of Marine Science and Engineering*, vol. 9, no. 2, pp. 194–221, 2021.

[7] H. Zong, J. Lyu, X. Wang, C. Zhang, R. Zhang, and X. Cai, "Grey box aggregation modeling of wind farm for wideband oscillations analysis," *Applied Energy*, vol. 283, Article ID 116035, 2021.

[8] W. Liu et al., "Frequency-coupled impedance model-based small-signal stability analysis of grid-tied converters under all operating conditions," *Zhongguo Dianji Gongcheng Xuebao/ Proceedings of the Chinese Society of Electrical Engineering*, vol. 40, no. 22, pp. 7212–7220, 2020.

[9] F. Hafiz, A. Swain, E. M. A. M. Mendes, and L. A. Aguirre, "MultiObjective evolutionary approach to grey-box identification of buck converter," *IEEE Transactions on Circuits and Systems I: Regular Papers*, vol. 67, no. 6, pp. 2016–2028, 2020.

[10] W. Hu, Z. Wu, and V. Dinavahi, "Dynamic analysis and model order reduction of virtual synchronous machine based microgrid," *IEEE Access*, vol. 8, pp. 106585–106600, 2020.

[11] N. Fulgêncio, C. Moreira, L. Carvalho, and J. Peças Lopes, "Aggregated dynamic model of active distribution networks for large voltage disturbances," *Electric Power Systems Research*, vol. 178, Article ID 106006, 2020.

[12] M. Amin and M. Molinas, "A grey-box method for stability and controller parameter estimation in hvdc-connected wind farms based on nonparametric impedance," *IEEE Transactions on Industrial Electronics*, vol. 66, no. 3, pp. 1872–1882, 2019.

[13] S. Lee, Y. B. Park, and Y. A. Jung, "Proposal of a verification method for embedded system design," *Journal of Advanced Research in Dynamical and Control Systems*, vol. 10, no. 1, pp. 199–207, 2018.

[14] S. Mat Zali and J. V. Milanovic, "Generic model of active distribution network for large power system stability studies," *IEEE Transactions on Power Systems*, vol. 28, no. 3, pp. 3126–3133, 2013.

[15] J. V. Milanovic and S. Mat Zali, "Validation of equivalent dynamic model of active distribution network cell," *IEEE Transactions on Power Systems*, vol. 28, no. 3, pp. 2101–2110, 2013.

[16] Y. Hu, S. Yurkovich, Y. Guezennec, and B. Yurkovich, "A technique for dynamic battery model identification in automotive applications using linear parameter varying structures," *Control Engineering Practice*, vol. 17, no. 10, pp. 1190–1201, 2009.

[17] M. R. Arahal, C. M. Cirre, and M. Berenguel, "Serial grey-box model of a stratified thermal tank for hierarchical control of a solar plant," *Solar Energy*, vol. 82, no. 5, pp. 441–451, 2008.

[18] A. M. Stanković and A. T. Sarić, "Transient power system analysis with measurement-based grey box and hybrid dynamic equivalents," *IEEE Transactions on Power Systems*, vol. 19, no. 1, pp. 455–462, 2004.

[19] M. V. Corrêa, L. A. Aguirre, and R. R. Saldanha, "Using steady-state prior knowledge to constrain parameter estimates in nonlinear system identification," *IEEE Transactions on Circuits and Systems I: Fundamental Theory and Applications*, vol. 49, no. 9, pp. 1376–1381, 2002.

[20] L. A. Aguirre, P. R. Donoso-Garcia, and R. Santos-Filho, "Use of a priori information in the identification of global nonlinear models- a case study using a buck converter," *IEEE Transactions on Circuits and Systems I: Fundamental Theory and Applications*, vol. 47, no. 7, pp. 1081–1085, 2000.

[21] W. H. Press, *Numerical Recipes in C*, Cambridge University Press, Cambridge, UK, 2nd edition, 1992.